# Elastic Scattering of 11.5—17.7-Mev Photons by Au Measured with a Bremsstrahlung Monochromator*†

J. S. O'Connell,‡ P. A. Tipler, and P. Axel
*Physics Department, University of Illinois, Urbana, Illinois*

(Received August 16, 1961; revised manuscript received December 19, 1961)

The external electron beam of the University of Illinois 25-Mev betatron and a post-bremsstrahlung electron spectrometer are used to provide a time coincidence which selects monochromatic photons with an energy resolution of 0.67%. For this resolution and an electron beam current of $3\times10^{-9}$ amp, the maximum photon intensity is about $1.5\times10^{5}$/sec for each electron detector placed in the spectrometer.

The elastic scattering of photons from Au was measured using the background limited intensity of $10^{4}$ photons/sec for each of the three electron detectors used simultaneously. The peak 135° differential scattering cross section was 0.71±0.05 mb/sr at 14.5 Mev. Other measured values at 135° were 0.11 (11.7 Mev), 0.32 (12.6 Mev), 0.67 (13.5 Mev), 0.54 (15.4 Mev), 0.38 (16.7 Mev), and 0.35 (17.6 Mev).

These scattering results would be in better agreement with photon absorption measurements if the absolute absorption cross sections were reduced by 9%. The results are consistent with dipole scattering, a cross section which varies smoothly with energy, and no high-energy inelastic scattering.

## I. INTRODUCTION

THIS paper describes the first elastic photon scattering experiments performed with the bremsstrahlung monochromator at the University of Illinois 25-Mev betatron. One of the aims of these experiments was to obtain information needed to improve the monochromator design and reduce possible sources of error. However, even with the equipment in a somewhat preliminary stage, the data compare favorably with those obtained by other techniques.

The Illinois bremsstrahlung monochromator is based on an extension of a technique first used by Weil and McDaniel[1] following the independent suggestions[1] of Koch and Camac. Similar work was reported recently by Cence.[2] Both experiments used the internal electron beam of an electron synchrotron. The first bremsstrahlung monochromator which used an extracted electron beam was the crude device tried by Goldemberg[3] at Illinois. Recently, a bremsstrahlung monochromator was employed with 1.75 Mev electrons.[4]

The present Illinois bremsstrahlung monochromator uses a time coincidence to identify the primary photon energy to within 0.67%, or 100 kev at 15 Mev. This is accomplished by using essentially monoenergetic electrons to produce bremsstrahlung in a thin converter which is in the conventional source position of a beta ray spectrometer. The degraded energy of an electron which has produced a photon in this converter is identified by the path the electron follows through the spectrometer. A time coincidence between the pulses produced by this energy degraded electron and by the scattered photon identifies the energy of the incident photon.

The operation of the monochromator is illustrated in Fig. 1 which shows how 15-Mev gamma rays can be selected. A monoenergetic beam of 20-Mev electrons impinges on the thin bremsstrahlung converter just below the center of Fig. 1. More than 99% of the original electron beam emerges from the converter without having produced any photons (of energy greater than 50 kev); this main beam is deflected by the spectrometer (as is shown by the heavy arrow head). The bremsstrahlung gamma rays proceed in a relatively narrow cone toward the scattering target. In Fig. 1, the spectrometer is adjusted so that 5-Mev electrons reach the electron detector in the lower left corner. Each of these electrons produced a 15-Mev photon (20-Mev incident electron minus 5-Mev residual electron). If one of these 15-Mev gamma rays interacts with the target and produces an event in the product detector (shown in the upper right hand corner of Fig. 1), the pulses from the electron detector and the product detector arrive at the proper time to activate the coincidence circuit (shown in the lower right corner). Thus, once chance

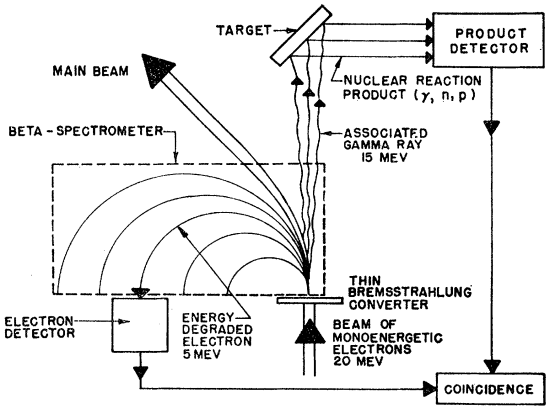


FIG. 1. Schematic of Bremsstrahlung Monochromator.

* The contents of this paper were submitted by J. S. O'Connell in partial fulfillment of the requirements for a Ph.D. in Physics.

† This research was supported in part by the joint program of the U. S. Office of Naval Research and the U. S. Atomic Energy Commission.

‡ Now at the Physics Department, Yale University, New Haven, Connecticut.

[1] J. W. Weil and B. D. McDaniel, Phys. Rev. **92**, 391 (1953).

[2] R. Cence, thesis and University of California Radiation Laboratory Report UCRL 8921 (unpublished).

[3] J. Goldemberg, Phys. Rev. **93**, 1426 (1954).

[4] M. Shea, R. Walter, and W. Miller, Bull. Am. Phys. Soc. **5**, 226 (1960).

coincidences have been subtracted, the only product detector events in coincidence with 5-Mev electrons are those produced by 15-Mev photons.

This paper describes the monochromator, its calibration with elastic scattering from the 15.1-Mev level in $C^{12}$, and its use in measuring the elastic scattering by $Au^{197}$ of gamma rays with energies between 11.5 Mev and 17.7 Mev. Section II describes the experimental arrangement briefly. Typical counting rates and the energy calibration and resolution as determined from the scattering of 15.1-Mev photons by $C^{12}$ are given in Sec. III. The experimental data obtained with $Au^{197}$ are given in Sec. IV, and these results are discussed and partially interpreted in Sec. V.

## II. MONOCHROMATOR OPERATION AND PERFORMANCE

The complete experimental arrangement is shown in Fig. 2. The primary electron beam, which is accelerated by the University of Illinois 25-Mev betatron[5,6] is extracted with the aid of a magnetostatic "peeler".[7] Each beam pulse has a duration of about 125 $\mu$sec[8]; with 180 pulses per sec this corresponds to a duty cycle of 2.2%. The beam is extracted symmetrically about the time at which the circulating electrons have their maximum energy so that the spread in energy of the emerging beam is only 0.33%. (This energy spread does not imply an equal uncertainty in photon energies.) The energy was kept relatively constant by using an electronic feedback circuit to stabilize the peak magnetic field in the betatron.

The extracted beam is focused by a pair of quadrupole magnets[9] to a 2 or 3 mm spot at the first focal point, $F_1$ (Fig. 2), about 2 m from the peeler. The bending or dispersion magnet accepts the slightly divergent beam from $F_1$, bends it through about 60°, and focuses on the converter at $F_2$ an image which should be about 1.5 times the image at $F_1$. The actual image is somewhat larger. The dispersion magnet is wedge shaped to produce horizontal focusing; vertical focusing is produced by the fringe field at entrance and exit.[10] The distance from $F_1$ to the entrance of the dispersion magnet is 2.5 m; it is 3.5 m from the exit to $F_2$.

The converter, located at the source position of an especially designed spectrometer,[11] was a brass foil, 4-cm wide, and 1-mil thick, corresponding to 1/600 radiation length. Multiple scattering of electrons in this thickness was small enough so that about 85% of 4-Mev electrons produced in the converter (or 68% of 3-Mev electrons) remained within the 8° acceptance cone of the spectrometer. A viewable scintillator was used periodically in the converter position to determine and check the electron beam position. The bremsstrahlung beam continues in the direction in which the main electron beam had been going when it hit the converter. In Fig. 2, the 5-in. diameter, 4-in. thick NaI gamma ray detector is shown intercepting this beam; this detector position is used to measure the number of monochromatic photons incident on the target. For a scattering measurement, the detector is placed at 135° with respect to beam; to reduce background, the detector was moved in a vertical plane while the spectrometer deflected electrons in a horizontal plane. The main electron beam left the spectrometer and hit a paraffin beam stopper.

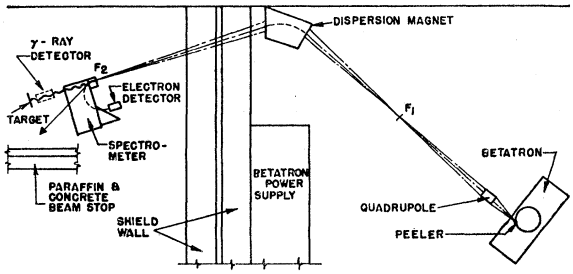


FIG. 2. Complete Experimental Arrangement.

The spectrometer focussed the energy degraded electrons on three electron detectors whose centers were about 2.5 cm apart. Each detector consisted of a Pilot B scintillator about 3.8 cm high, 0.8 cm thick, and 1.4 cm wide; in the spectrometer, this width would accept electrons in an interval of 1.5% $E_e$ where $E_e$ is the energy of the post-bremsstrahlung electron. Each scintillator was surrounded by aluminum which reflected the emitted light to the photosurface of an RCA 6810A photomultiplier.

The dispersion magnet spread the beam at the converter according to the energy of the incident electrons $E_\beta$; the dispersion $(dE_\beta/E_\beta dx)$ was 0.24%/cm. The spectrometer had an energy dispersion $(dE_e/E_e dx)$ of 1.06%/cm. Therefore, if the monochromator was operated with dispersion and spectrometer magnets set for $E_\beta = 4.4\ E_e$, these two dispersions compensated to produce a unique gamma ray energy $E_\gamma$ independent of fluctuations in $E_\beta$. However, when other ratios of $E_\beta/E_e$ were used, the energy spread in $E_\beta$ produced a small energy spread in $E_\gamma$. The magnetic fields of the magnets were measured with temperature compensated Halltron HR31 Hall effect probes.

The electronic circuits were designed[12] both to sense coincidences between post-bremsstrahlung electrons and

[5] D. W. Kerst, Rev. Sci. Instr. **13**, 387 (1942).
[6] D. W. Kerst, *Encyclopedia of Physics*, edited by S. Flugge, (Springer-Verlag, Berlin, 1959), Vol. XLIV.
[7] L. Skaggs, G. Almy, D. Kerst, and L. Lanzl, Phys. Rev. **70**, 95 (1946).
[8] T. J. Keegan, Rev. Sci. Instr. **24**, 472 (1953).
[9] E. D. Courant, M. S. Livingston, and H. S. Snyder, Phys. Rev. **88**, 1190 (1952); see also M. Livingston, *High-Energy Accelerators* (Interscience Publishers, Inc., New York, 1954) for a discussion of the design of "The A-G Magnetic Lens."
[10] W. Cross, Rev. Sci. Instr. **22**, 717 (1951).
[11] J. S. O'Connell, Rev. Sci. Instr. **32**, 1314 (1961).
[12] We are indebted to Dr. D. Jamnik, Ljubljana, Yugoslavia who designed and tested the transistorized electronic system used to detect coincidences and to provide a gated pulse proportional to the energy of the detected photon.

photons, and to display a crude energy spectrum of the coincident photons. Pulses from the anode of the electron detector photomultipliers were limited and applied to one input of a diode coincidence circuit. The other input to each coincidence circuit came from the RCA 7046 photomultiplier which viewed the NaI scintillator. These photon pulses were first discriminated, then amplified by a distributed line amplifier, and finally limited and clipped to about 8 nanoseconds (m$\mu$sec) before they reached the coincidence circuit.

The electron anode pulses were clipped to a few nanoseconds with shorted cable. The gamma anode pulses were shortened at the detector by using a 5m shorted cable to avoid pile-up in the amplifier preceding the coincidence circuit. The coincidence delay curves had a full width of about 10 m$\mu$sec at half maximum. Three coincidence circuits were used for the three detectors, and a fourth circuit, with an extra delay cable inserted to destroy the match in timing, was used to record chance coincidences.

If any one coincidence circuit was activated, a 100 m$\mu$sec rectangular voltage waveform activated a diode gate circuit which allowed the photon dynode pulse to proceed through a slow (i.e., 1 $\mu$sec) amplifier. This gating was accomplished after the dynode pulse had been amplified to about 2 v. After the somewhat stretched gated dynode pulse had been amplified further, it was added to a pedestal voltage characteristic of the particular coincidence circuit which had been activated. (If two coincidence circuits were activated within the 100 m$\mu$sec interval, both pulses were rejected.) The resultant pulse amplitude was analyzed by (and stored in) an RIDL 100 channel analyzer which, with the aid of the pedestals, was being used as four 25 channel analyzers. Each group of 25 channels recorded a spectrum of photons; the first three groups corresponded to the three electron detectors while the fourth group gave the chance coincidence background. The total number of pulses from one electron detector were counted continuously with a fast scaler.

## III. TYPICAL COUNTING RATES AND CALIBRATION USING THE 15.1-MEV LEVEL IN $C^{12}$

### A. Relation between Cross Section and Measured Counting Rate

The elastic scattering cross section can be obtained rather directly by measuring the number of scattered gamma rays for a recorded number of electrons of definite energy. Two auxiliary measurements are needed at each new energy in order to determine (a) the number of monochromatic gamma rays which strike the target, and (b) the number of chance coincidences.

The number of true counts, $N_t$, due to elastically scattered monochromatic gamma rays depends on: (1) the number of energy degraded electrons, $N_e$, which give a detectable pulse in the electron detector, (2) the probability, $P_\gamma$, that the monochromatic gamma ray associated with the detected electron strikes the target, (3) the average transmission of the incident gamma rays, $T_{\text{in}}$, and the transmission of the scattered gamma rays en route to the detector, $T_0$, (4) the number of target atoms per cm$^2$, $\mathfrak{N}$, perpendicular to the gamma ray beam, (5) the differential scattering cross section, $d\sigma/d\Omega$, (6) the geometric solid angle subtended by the detector, $\Omega_{dg}$, and (7) the efficiencies of both the photon detector, $F_d$, and the electronic circuits, $F_e$.

$$N_t = N_e P_\gamma T_{\text{in}} \mathfrak{N} (d\sigma/d\Omega) T_0 \Omega_{dg} F_d F_e. \tag{1}$$

It is convenient to define the effective number of gamma rays, $N_{\gamma\text{eff}}$, the effective solid angle, $\Omega_d$, and the effective number of target atoms/cm$^2$, $\mathfrak{N}_{\text{eff}}$, with the aid of a constant $c$ which will be defined in Eq. (7):

$$N_{\gamma\text{eff}} = N_e P_\gamma F_d F_e / c, \tag{2}$$

$$\Omega_d = c\Omega_{dg}, \tag{3}$$

$$\mathfrak{N}_{\text{eff}} = \mathfrak{N} T_{\text{in}} T_0. \tag{4}$$

In terms of these quantities, the relation between the observed counting rate and the desired cross section is:

$$N_t = N_{\gamma\text{eff}} \mathfrak{N}_{\text{eff}} (d\sigma/d\Omega) \Omega_d. \tag{5}$$

The precision with which $d\sigma/d\Omega$ could be obtained from Eq. (5) would be seriously limited by uncertainties about factors appearing in $N_{\gamma\text{eff}}$ if it were not for an auxiliary experiment in which the identical gamma ray detector is placed in the bremsstrahlung beam to record monochromatic photons of the correct energy. Using the subscript $b$ to denote quantities measured in this auxiliary experiment:

$$N_{tb} = N_{eb} P_{\gamma b} F_{db} F_{eb}. \tag{6}$$

It is now possible to obtain a directly measurable expression for $N_{\gamma\text{eff}}$ by defining $c$ properly:

$$c = (P_\gamma / P_{\gamma b})(F_d / F_{db})(F_e / F_{eb}), \tag{7}$$

$$N_{\gamma\text{eff}} = N_e (N_{tb} / N_{eb}). \tag{8}$$

The correction factor, $c$, which is somewhat less than 1, can be calculated; it can then be used to calculate the effective solid angle, $\Omega_d$, from Eq. (3).

The contribution to $c$ from $(P_\gamma/P_{\gamma b})$ could be made negligible by setting a collimating aperture equal to the target size in the target position while measuring $(N_{tb}/N_{eb})$. The target was 4 in. wide and 5.5 in. high tilted to subtend a 4 in. square perpendicular to the beam; it was about 6 ft. from the bremsstrahlung converter. The front face of the NaI detector was 7.5 in. from the target position whether scattering or bremsstrahlung was being measured. (The fraction of the gamma rays eliminated by the aperture was small enough so that measurements without an aperture at some energies could be corrected using data with and without apertures at other energies; this procedure avoided the trouble of setting up the aperture at each

energy and was adequate for the statistical accuracy achieved.)

Two precautions were taken to be sure that the electronic efficiencies, $F_e$ and $F_{eb}$, were identical. First, the relevant pulse heights were kept the same by adjusting the high voltage gain to compensate for the slight gain shift due to the fringe magnetic field present at the detector when it was in the scattering position. Second, the electron and photon counting rates were kept low enough so that the electronic circuits would perform reliably independent of the rates. When the gamma ray detector was placed in the primary photon beam, the beam intensity was reduced three or four orders of magnitude to guard against possible gamma ray pile up or phototube fatigue. The electron counting circuits operated reliably at rates above the typical $N_e=10^4$/sec used in most scattering experiments.

The main corrections in $c$ are due to the difference between the crystal efficiencies, $F_d$ and $F_{db}$, caused by the larger divergence of the scattered gamma rays. Using the results of Monte Carlo calculations described by Miller and Snow,[13,14] we found that $c=0.69$, if one interprets $\Omega_{dg}$ as the physical solid angle which the front face of the crystal subtends at a point on the crystal axis at the position of the target. (These calculations show if that 15-Mev gamma rays are emitted isotropically from a point on the axis of a 5-in. diameter crystal 7.5 in. from the front face, the interaction probability is about 76% of that expected if the gamma rays which hit the front face were incident parallel to the crystal axis. There is also a factor of 0.98 to account for reduction in solid angle due to the extended size of the sample, and a factor of 0.93 due to the smaller fraction of the interacting gamma rays which leave enough energy in the crystal to be included with the elastic events.)

The desired cross section can be expressed in terms of measured quantities except for the value of $c$ contained in $\Omega_d$:

$$\frac{d\sigma}{d\Omega}=\frac{1}{\mathfrak{N}_{\text{eff}}}\frac{N_t}{N_e}\frac{N_{eb}}{N_{tb}}\frac{1}{\Omega_d}=\frac{1}{\mathfrak{N}_{\text{eff}}}\frac{N_t}{N_{\gamma\text{eff}}}\frac{1}{\Omega_d}. \tag{9}$$

The experiments described below used a tilted 4-in. wide by 5.5-in. high sample which subtended a 4-in. square of the beam, this target was parallel to and 7.5 in. from the 5-in. diameter NaI crystal. For this arrangement, $\Omega_d=0.227$ sr. Only if much more precise determinations were being attempted would it be necessary to refine $c$ in order to include the slight energy dependence or the slight change in relative efficiency caused by the $\frac{1}{2}$-in. Al and $\frac{1}{8}$-in. Pb beam cleaners which were always in front of the NaI crystal.

In the data reported below, $N_t$ was obtained by subtracting the chance coincidence background from the observed number of coincidences. $N_e$, $N_{eb}$, and $N_{tb}$ were measured directly. $\mathfrak{N}_{\text{eff}}$ for Au was calculated using known atomic absorption coefficients; for quantitative interpretation of the counting rates due to a single strong nuclear level, such as encountered in $C^{12}$, it would be necessary to include the resonant nuclear absorption[15,16] together with the atomic absorption.

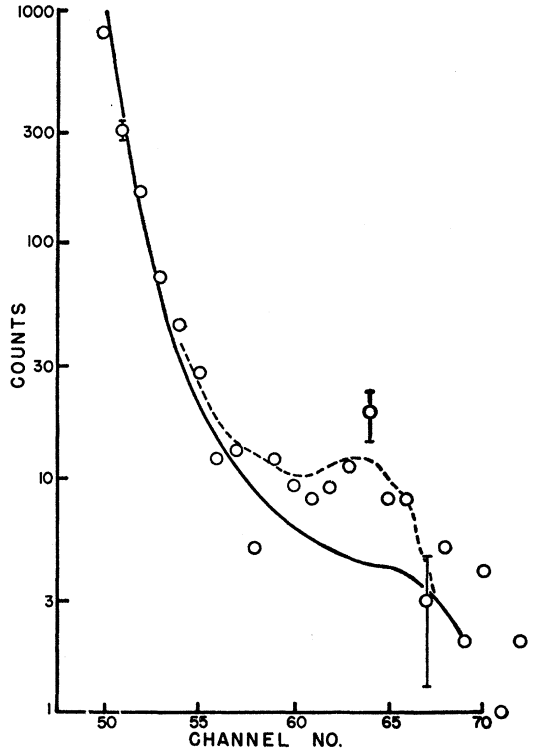


FIG. 3. Typical Scattering Data. The number of detected scattered monochromatic gamma rays (12.64 Mev) is plotted on a logarithmic scale as a function of energy. Channel 50 corresponds to about 5 Mev, while channel 63 corresponds to about 12.5 Mev. The solid curve is the chance coincidence background; the dashed curve is drawn to emphasize the trend of the experimental data.

## B. Typical Data

The observed data due to the scattering of 12.64-Mev gamma rays by Au are shown in Fig. 3. The open circles give the observed counting rates; the logarithmic ordinate scale indicates the total number of counts while the abscissa indicates the channel number which is equivalent to pulse height or energy. The smallest accepted pulses appear in channel 50 and correspond to about 5 Mev. Each channel includes about a 0.6-Mev energy interval, and the 12.64-Mev counts of interest are centered in channel 63. The dashed line is drawn merely to emphasize the trend of the data.

The heavy black curve is a rather precise measure of the chance coincidence background which is determined

[13] W. Miller and W. Snow, Rev. Sci. Instr. **31**, 39 (1960); see also Argonne National Laboratory Report ANL 6310 (unpublished).

[14] We are indebted to W. Miller and W. Snow who kindly performed these calculations for the geometries we needed.

[15] Evans Hayward and E. G. Fuller, Phys. Rev. **106**, 991 (1957).

[16] E. L. Garwin, Phys. Rev. **114**, 143 (1959); see also S. S. Hanna and R. E. Segel, Proc. Roy. Soc. (London) **A259**, 267 (1960).

with the aid of the fourth coincidence circuit. The input cables to this fourth coincidence circuit are purposely adjusted, so that truly coincident pulses will not arrive simultaneously; this circuit therefore measures only chance coincidences. This measured chance coincidence rate is then used to find the number of chance coincidences in the three true coincidence channels.

The origin and the measurement of the chance coincidence background can be illustrated by considering a typical electron counting rate of 50 counts per electron detector per betatron pulse. Consider a single electron detector, each of whose pulses makes its coincidence circuit sensitive for 10 nanoseconds. Due to the 50 events per pulse, each coincidence circuit would be sensitive for 0.5 $\mu$sec during each pulse. If the pulse has an average duration of 100 $\mu$sec, the 0.5 $\mu$sec sensitivity implies that there is 1 chance in 200 that any gamma ray pulse large enough to activate the coincidence circuit will find the coincidence circuit activated by an unrelated electron. It is necessary to measure the chance coincidence background continuously, because the factor given as 1 in 200 in the example above depends on the average value of the square of the instantaneous beam intensity. The measured chance coincidence rate automatically takes into account fluctuations of the beam intensity during a run, or even during a single beam pulse. The factor of 200 can be thought of as a "singles rejection ratio" because if there are 200 single gamma rays counts that are not in coincidence, the coincidence circuit allows only one to be recorded.

The chance coincidence background shown by the heavy line in Fig. 3 is deduced from two measurements. The vertical position of this line (which is governed by the singles rejection ratio) is found from the fourth coincidence circuit which records only chance coincidences. This quantity can be determined quite precisely with the aid of the numerous low energy gamma rays. The shape (or energy distribution) of the chance coincidence background is determined by an auxiliary "singles" measurement in which the electron side of the coincidence circuit corresponding to the group of channels from 50 to 75 is biased so that every gamma ray pulse is recorded.

A very convenient check was used in each run to assure the correctness of the determined chance coincidence background. The relative slowness of the pulses from the gamma ray detector corresponds to an apparent delay in the gamma ray pulses; this delay varies inversely with pulse amplitude. Because of this effect, if the cable lengths are adjusted to record coincidences due to high-energy gamma rays, the delays will be incorrect for low-energy gamma rays. Therefore, even if some low-energy gamma rays were actually in coincidence with electrons, they would not activate the coincidence circuit soon enough to be recorded. This implies that all of the recorded coincidences due to low-energy gamma rays must be due to chance coincidences, and that the curve corresponding to the chance coincidence background must go through the experimental low-energy gamma ray points. It never required more than a fraction of a channel shift of the coincidence curve relative to the singles curve to have the two overlap with the singles rejection ratio determined from the chance coincidence channel. This relative shift never produced a significant change in the implied number of true coincidences.

Once the chance coincidence background is known, the true coincidence counting rate can be computed easily. In Fig. 3 there are 55 total counts in the five channels from 61 to 65. (Only the channels near the peak are accepted in an attempt to minimize the errors that could be introduced by slight shifts in gain. For example, the apparent true counting rate between channels 55 and 60 could be changed by a significant factor by a half channel shift of the chance background curve.) Of the 55 observed counts, 27.3 are attributable to chance background. The true number of counts, $N_t$, is therefore taken as $27.7\pm\sqrt{55}$; the error in the 27.3 chance counts is negligible (because both the singles rejection ratio and the energy distribution of the gamma ray pulses are known relatively precisely).

The scattering data obtained at 12.64 Mev (in Fig. 3) was chosen as a sample spectrum to illustrate the reliability of an experimental determination despite both the relatively small number of significant events and the relatively large chance background. For many of the other experimental points the number of true events was large enough to show clearly the effective response of the detector to essentially monochromatic gamma rays.

In order to determine the differential scattering cross section, $d\sigma/d\Omega$, (from Eq. 9), it was necessary to find $N_{\gamma\,\mathrm{eff}}$ by measuring the monochromatic gamma rays detected by the NaI scintillation crystal when it intercepts the primary bremsstrahlung beam [i.e., with the aid of Eq. (8)]. Typical data obtained with the gamma ray detector in the bremsstrahlung position are shown in Fig. 4; this graph displays $N_{tb}$ of Eq. (6). Gamma rays in about a 130-kev interval about 12.78 Mev are shown by the curve in the group of channels from 0 to 25. The broadness of the peak indicates the poor energy resolution obtained with time shortened pulses from NaI. The pulses in channels 48–72 are due to 12.64-Mev photons; the highest group of channels correspond to gamma ray energy of 12.50 Mev. (The higher number of counts in this highest group of channels was due to minor differences in coincidence efficiency due to different effective electronic biases.) During a single bremsstrahlung run only three of the four spectra shown in Fig. 4 would appear; the pulses between channels 25 and 48 would not appear because the timing of the corresponding coincidence circuit is adjusted so that it will record only chance coincidences. The data shown in channels 25–48 were obtained with an auxiliary measurement during which an extra delay cable was inserted.

The effective number of gamma rays per detected

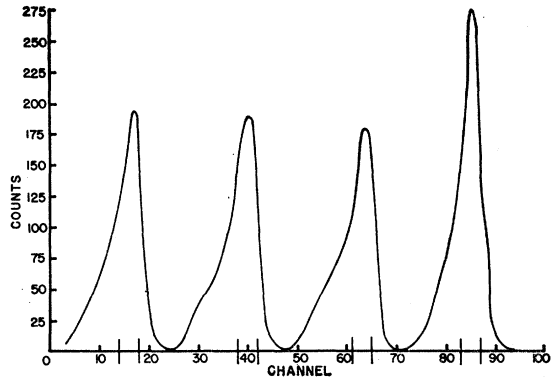


FIG. 4. Pulse Height Spectra Produced by Monochromatic Gamma Rays. Four different pulse height distributions are displayed simultaneously in the 100 channel analyzer. Channels 1–24 correspond to the system response when 12.78 Mev gamma rays strike the NaI; Channels 25–48 and 49–72 are used for 12.64 Mev gamma rays, and 72–95 are used for 12.50 Mev gamma rays. The differences in the spectra are due to differences in the electronic biases in the four coincidence circuits and the following circuitry. The vertical lines on the horizontal axis show the four intervals whose counts were used to measure the intensity of the incident and scattered gamma rays; the remainder of the spectrum was not used because it contains large chance coincidence contributions when scattered radiation is detected (as in Fig. 3).

electron (i.e., $N_{tb}/N_{eb}$) was different for the different counters and also varied from run to run. On the average, the four coincidence channels had relative efficiencies of 1.00, 1.04, 0.97, and 1.30. There was a systematic increase in $N_{tb}/N_{eb}$ as the incident electron energy increased as would be expected from the decreased divergence of the primary photon beam for higher primary electron beam energies. The increased absorption of higher energy gamma rays by NaI also probably contributed to this. Superimposed on these systematic fluctuations were some anomalies which could have been due to variations in electronic biases. In only one series of runs (at 15.4 Mev) did the ratio $N_{tb}/N_{eb}$ vary for all detectors in a way that would have been consistent with an improper position of the electron beam on the converter. (The apparent average ratio, $N_{tb}/N_{eb}$ was 20% below its value at neighboring energies.) The same effect could more likely have been produced by some electronic anomaly which persisted throughout the particular scattering measurement. The data were analyzed using this assumption, and this interpretation was partially confirmed by the way in which the 15.4-Mev point fit together with the other points (i.e., the 15.4-Mev point would fit much more poorly if the cross section were reduced by 20%).

The average value of $N_{tb}/N_{eb}$ was about 0.1 implying that when the NaI was in the bremsstrahlung beam, 1 monochromatic gamma ray was detected in coincidence for each 10 detected electrons. This factor of 0.1 arises because (1) only about 50% of the photons were intercepted by the 5-in diameter NaI detector which was about 2 m from the converter, and (2) only about 20% of the incident photons produced a usable coincidence count. (This 20% efficiency can be explained approximately as follows: (a) about 75% of the incident photons were transmitted through the $\frac{1}{2}$-in. Al and $\frac{1}{8}$-in. Pb absorbers used in front of the detector to attenuate very low energy photons, (b) about 60% of the photons which reach the crystal interact, and (c) about 45% of the interactions give pulses of usable amplitude, activate the coincidence circuit, and appear in the preselected high energy part of the NaI pulse spectrum. The preselected channel intervals are shown by the vertical lines along the channel axis in Fig. 4.)

### C. Typical Counting Rates

The achievable counting rates depend on a variety of experimental conditions rather than on the available electron intensity alone. For scattering by the continuum of levels in the electric dipole giant resonance, the counting rate is limited by the chance coincidence background which limits the usable size of the primary electron beam. Considerably higher counting rates can be obtained from scattering by some isolated resonances in light nuclei because higher beam intensities can be used.

Consider first values typical of elastic scattering in the giant dipole resonance of heavy nuclei. When the detector is at 135° with respect to the beam, the background comes mainly from the target. (To reduce the background due to the main beam, it was necessary to produce the 135° displacement of the gamma ray detector in a vertical plane. The main electron beam emerged from the spectrometer deflected in the horizontal plane.) A substantial fraction of the residual, target-produced background, if not all of it, is nuclear in origin. There might be of the order of 100 scattered non-monochromatic gamma rays for each scattered monochromatic gamma ray (in a 100-kev interval). If chance-to-true ratio is to be kept as low as 1 to 2, the probability of a non-monochromatic gamma ray forming a coincidence must be kept as low as 1 in 200. As indicated in III-B above, a value of 1 in 200 corresponds to 50 detected electrons in a 100 $\mu$sec pulse. (The usable electron beam is thereby limited except insofar as the beam pulse can be increased in duration or insofar as the resolving time can be decreased.) For most of the experiments with an Au target, the electron counting rate in each detector was adjusted to about $8\times10^3$/sec by varying the primary electron beam intensity. Since the value of $N_{tb}/N_{eb}$ is within 20% of 0.1, $N_{\gamma\text{eff}}$ was about $8\times10^{+2}$/sec.

The effective number of atoms/cm$^2$ in the 1 kg Au target was within 3% of $2.07\times10^{22}$ atoms/cm$^2$ for all energies. (The target had a surface density of 7.61 gm/cm$^2$, and at its inclination presented $3.29\times10^{22}$ atoms/cm$^2$ perpendicular to the incoming beam. The calculated atomic absorption reduced this by from 35% to 39%. These absorption calculations interpolated between Pt and Pb in the tables given by Grodstein,[17]

[17] G. W. Grodstein, National Bureau of Standards Circular 533, 1957 (unpublished).

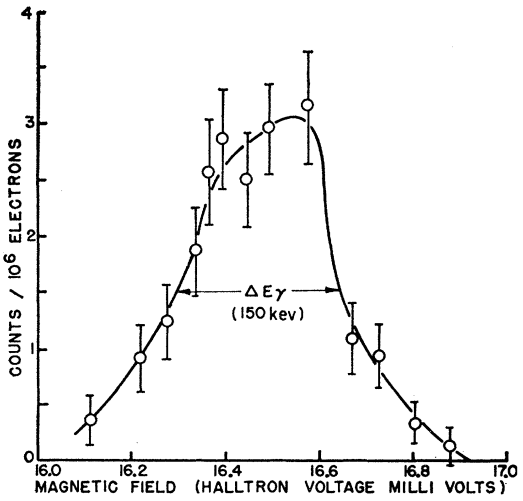


FIG. 5. Energy Resolution of System for Monochromatic 15.1-Mev Gamma Rays. The detected counts (per million electrons) due to the scattering of 15.1-Mev gamma rays by $C^{12}$ is plotted as a function of the post-bremsstrahlung electron spectrometer setting for a constant energy of incident electrons. The abscissa is the magnetic field of the spectrometer as measured by the Hall voltage (in millivolts) on the Halltron probe. The electron energy was about 7 Mev and the full width at half maximum was 150 kev.

using total absorption coefficients. The attenuation due to atomic absorption is overestimated insofar as some of the forward Compton scattering would not eliminate the gamma rays; as partial compensation, the attenuation estimates omit nuclear absorption. A 2% increase in the true total absorption coefficient would produce about a 1% decrease in the effective number of atoms.)

The estimates given ($\Omega_d=0.227$ sr, $N_{\gamma\text{eff}}=8\times10^2$/sec, and $\mathfrak{N}_{\text{eff}}=2.07\times10^{22}$) show that for a differential cross section of 0.35 mb/sr (which is half of the peak value) the typical counting rate was 4.7 counts/hr for each of the three electron detectors which were used simultaneously.

There are four factors which increase the counting rate significantly when elastic scattering from the 15.1-Mev level in carbon is measured. Since the scattering cross section (differential in angle at 135° but integrated over energy) is 0.21 Mev-mb/sr, the apparent average cross section with 150-kev resolution is about 1.4 mb/sr, which is four times the value used to estimate the 4.7 counts/hr above. An effective target thickness of $10^{23}$ atoms/cm$^2$ can be used; this factor of 5 is not available with heavier targets like Au due to atomic absorption. An additional factor of 1.6 can be obtained because the lower background makes it possible to use a larger fraction of the pulse heights produced by the 15-Mev gamma ray in the NaI. This lower background also has the more important effect of making it possible to use much higher beam currents. (The current can be increased easily by a factor of 20 above the $1.6\times10^{-10}$ amp typical for $8\times10^3$ electrons/second/100 kev. However for the carbon experiment reported below, the current was not increased significantly, and counting rates of about 150/hr were used.)

### D. $C^{12}$ Calibration Experiment

The 15.1-Mev gamma rays scattered by $C^{12}$ were measured to provide an accurate energy calibration and to exhibit the energy resolution of the system.

Figure 5 shows the coincidence counting rate for one of the electron detectors as a function of the current in the electron spectrometer. For this measurement the incident electron beam had an energy of 22.02 Mev while the post-bremsstrahlung electrons had energies of about 7 Mev. The observed full width at half maximum of about 150 kev was due to (a) the finite width of the electron detector which corresponded to about 110 kev for the 7-Mev electrons, (b) the finite electron spot size at the converter which contributed a spread of about 50 kev because $E_\beta/E_e$ was set at about 3.1 rather than 4.4. (Resolution curves with about 100 kev full width at half maximum have been obtained more recently using $E_\beta=19.5$ Mev and $E_e=4.4$ Mev.)

The energies $E_\beta$ and $E_e$ were determined by measuring the magnetic fields of the dispersion and spectrometer magnets respectively with the aid of the Hall effect probes. The two magnets were intercalibrated by removing the bremsstrahlung converter so that the main electron beam which had passed through the dispersion magnet could be deflected into one of the electron detectors at the output of the spectrometer magnet; there was a linear relation between the two magnets. The energy of the electrons was known crudely from the available calibration of the Illinois 25-Mev betatron. When this energy calibration was used as a guide, the Hall effect probe readings appeared to depend linearly on the energy. The value of $E_\beta-E_e$ at which the 15.1-Mev $C^{12}$ scattering was observed was taken as an absolute energy of 15.12 Mev, corresponding to the excitation of $15.11\pm0.01$-Mev level[18] in $C^{12}$.

## IV. DATA FROM THE SCATTERING OF PHOTONS BY Au

The experimental data obtained are summarized in Table I and Fig. 6. Column I of Table I gives the 21 different photon energies obtained with the seven different settings of $E_\beta$ (given in column II) each of which was used with three values of $E_e$. In the entire series of measurements $E_e$ for the center electron detector varied between 4.30 Mev and 6.55 Mev. The center electron counter was used for the chance coincidence determination (i.e., this counter corresponded to the gamma ray energies 11.66 Mev, 12.64 Mev, etc.). Column III gives the effective number of gamma rays; the number of counted electrons was about 10 times larger. The counting rate corresponded to about 800 effective gamma rays per sec. The total time during which scattering data

[18] F. Ajzenberg-Selove and T. Lauritsen, Nuclear Phys. 11, 1 (1959).

TABLE I. Experimental results.

| $E_\gamma$ Mev | $E_\beta$ Mev | $N_{\gamma\text{eff}}$ $10^7\times$ | Total Counts | Chance Counts | $d\sigma/d\Omega$ $10^{-28}$ cm²/sr Individual | Average |
|---|---|---|---|---|---|---|
| 11.48 | | 2.06 | 20 | 12.0 | 0.80±0.45 | |
| 11.66 | 18.03 | 1.64 | 21 | 9.7 | 1.41±0.58 | 1.07±0.30 |
| 11.84 | | 1.61 | 15 | 7.1 | 1.00±0.50 | |
| Chance | | 1.70 | 9 | 7.5 | | |
| 12.50 | | 2.66 | 72 | 33.2 | 3.02±0.66 | |
| 12.64 | 18.03 | 1.95 | 55 | 27.3 | 2.94±0.79 | 3.18±0.43 |
| 12.78 | | 2.15 | 57 | 19.9 | 3.57±0.73 | |
| Chance | | 2.15 | 23 | 24.5 | | |
| 13.30 | | 1.39 | 53 | 12.2 | 6.14±1.1 | |
| 13.45 | 19.83 | 1.11 | 40 | 9.0 | 5.83±1.2 | 6.73±0.71 |
| 13.62 | | 1.15 | 53 | 7.8 | 8.21±1.4 | |
| Chance | | 1.10 | 8 | 8.6 | | |
| 14.30 | | 3.07 | 134 | 29.2 | 7.20±0.80 | |
| 14.44 | 19.83 | 2.27 | 107 | 19.2 | 8.18±0.97 | 7.12±0.52 |
| 14.58 | | 2.28 | 87 | 22.3 | 5.99±0.87 | |
| Chance | | 2.06 | 18 | 23.0 | | |
| 15.29 | | 1.94 | 104 | 48.0 | 6.11±1.1 | |
| 15.41 | 19.83 | 1.44 | 66 | 26.6 | 5.80±1.2 | 5.45±0.66 |
| 15.53 | | 1.48 | 61 | 29.9 | 4.45±1.1 | |
| Chance | | 1.34 | 32 | 28.8 | | |
| 16.55 | | 0.820 | 22 | 5.6 | 4.30±1.3 | |
| 16.69 | 22.02 | 0.564 | 14 | 4.6 | 3.59±1.5 | 3.83±0.78 |
| 16.83 | | 0.623 | 15 | 4.6 | 3.59±1.4 | |
| Chance | | 0.668 | 7 | 4.8 | | |
| 17.48 | | 0.882 | 17 | 12.6 | 1.08±1.05 | |
| 17.60 | 22.02 | 0.631 | 16 | 5.5 | 3.59±1.35 | 3.48±0.80 |
| 17.72 | | 0.622 | 24 | 7.4 | 5.78±1.7 | |
| Chance | | 0.666 | 7 | 5.6 | | |

were being collected was about 50 hours. During a standard run (i.e., when no major equipment problems arose), between one and two hours of setup, calibration, and auxiliary experiments seem to be required for each hour devoted to the actual scattering measurement.

The total number of observed coincidence counts are given in column IV while the inferred number of chance coincidence counts are given in column V. The statistical error associated with the number of net or true coincidence counts is the square root of the number in column IV (as explained in Sec. IIIB, above). The differential scattering cross sections, as calculated from Eq. (9), are given in column VI and are plotted in Fig. 6. Only the statistical errors are shown. There might be additional errors of about 10% due to unknown fluctuations in $N_{tb}/N_{eb}$, and 10% in the absolute cross section. (The effective value of the $N_{tb}/N_{eb}$ could shift if the beam shifted its position on the converter; however, aural monitoring of the electron counting rate kept such fluctuations low. The measurement of $N_{tb}/N_{eb}$ depended on the beam position remaining relatively constant when the beam intensity was reduced in order to make the measurement.)

The energy resolution for the different points is not known exactly because some of the points were taken with a somewhat defocussed spot (i.e., an electron spot size of more than 7 mm on the converter.) Throughout the experiment, the resolution was probably 150±30 kev. The data in Fig. 6 are shown with a uniform resolution of 150 kev; the actual resolution was probably somewhat greater than 150 kev for 11.7 Mev, 13.5 Mev, and 16.7 Mev while the resolution was somewhat less for the other four sets of points.

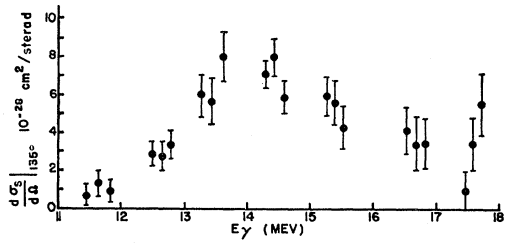


FIG. 6. Differential Scattering Cross Section of $Au^{197}$ at 135°. The cross section includes both elastic scattering and high energy inelastic scattering. The ordinate is the differential cross section in units of $10^{-28}$ cm²/sr; the abscissa is the gamma ray energy in Mev. The energy resolution varied from point to point but was about 150 kev±30 kev.

Figure 6 shows no evidence for rapid energy variation of the cross section. Despite the limited statistical accuracy, the absence of structure is significant because there have not been any other photon experiments with comparable energy resolution.

Due to the limited statistical accuracy, the data from the three neighboring electron detectors were combined to give the results shown in column VII of Table I. These data correspond to resolutions of from about 270 kev to about 450 kev depending on the values of $E_e=E_\beta-E_\gamma$.

## V. COMPARISON OF SCATTERING AND ABSORPTION MEASUREMENTS

### A. Dispersion Relations

The differential elastic scattering cross section in the forward direction, $d\sigma_s(0°)/d\Omega$, can be obtained from the forward scattering amplitude, $f$.

$$d\sigma_s(0°)/d\Omega=|f|^2. \tag{10}$$

The imaginary part of $f$, Im $f$, is related to the total interaction cross section by the optical theorem; for the giant resonance region where the absorption cross section, $\sigma_a$, is essentially equal to the total cross section:

$$\text{Im } f=\sigma_a(E)/4\pi\lambda\!\!\!^{-}. \tag{11}$$

The real part of $f$, Re $f$, is related to the imaginary part of $f$ by the dispersion relation[19]:

$$\text{Re}f(E)=\text{Re}f(0)+\frac{2E^2}{\pi}P\int_0^\infty dE'\frac{\text{Im}f(E')}{E'(E'^2-E^2)}, \tag{12}$$

where Re $f(0)$ is the Thomson scattering amplitude, $-Z^2e^2/AMc^2$, of a nucleus with charge $Ze$ and mass $AM$ (where $M$ is the nucleon mass), and where $P$ stands for the Cauchy principal value of the integral. Using

[19] M. Gell-Mann, M. L. Goldberger, and W. E. Thirring, Phys. Rev. **95**, 1612 (1954).

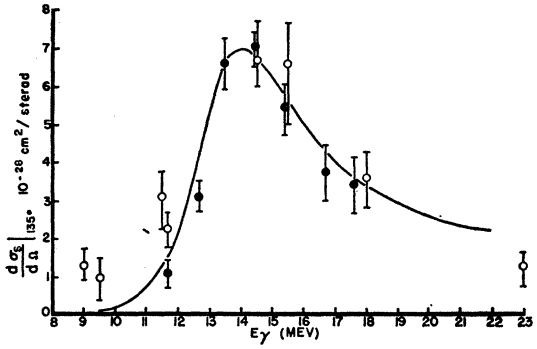


FIG. 7. Differential Scattering Cross Section for $Au^{197}$ at 135°. The experimental dots (this experiment) and open circles (0.82 times the adjusted value obtained from references 23 and 24) may include high energy inelastic scattering; the solid curve is 0.82 times the prediction for only elastic scattering obtained by using published value of measured absorption cross section (reference 21). The energy resolution varies from point to point but is about 350 kev.

Eq. (11), Eq. (12) can be rewritten as:

$$\mathrm{Re}f(E)=-\frac{Z^2e^2}{AMc^2}+\frac{E^2}{2\pi^2\hbar c}P\int_0^\infty dE'\frac{\sigma_a(E')}{E'^2-E^2}. \quad (13)$$

The integral has a simple value [20] when $\sigma_a(E)$ has a Lorentz shape:

$$\sigma_a(E)=\frac{\sigma_m}{[(E_0^2-E^2)/E\Gamma]^2+1}\equiv\frac{\sigma_m}{L^2+1}. \quad (14)$$

where $\sigma_m$ is the maximum value of the absorption cross section. In this case,

$$\mathrm{Re}\, f(E)=-(Z^2e^2/AMc^2)+L\ \mathrm{Im}\ f(E). \quad (15)$$

Substituting Eqs. (15) and (11) in Eq. (10) gives:

$$\frac{d\sigma_s(0°)}{d\Omega}=\frac{\sigma^2{}_m}{(4\pi\lambda\!\!\!^{-})^2}\left\{\left[\frac{1}{L^2+1}\right]^2+\left[\frac{L}{L^2+1}-\frac{Z^2e^2 4\pi\lambda\!\!\!^{-}}{AMc^2\sigma_m}\right]^2\right\}. \quad (16)$$

If $\sigma_a(E)$ can be represented by $n$ Lorentz lines, Eq. (16) becomes:

$$\frac{d\sigma_s(0°)}{d\Omega}=\frac{1}{(4\pi\lambda\!\!\!^{-})^2}\left\{\left[\sum_{i=1}^{n}\left(\frac{\sigma_{mi}}{L_i^2+1}\right)\right]^2+\left[\sum_{i=1}^{n}\left(\frac{\sigma_{mi}L_i}{L_i^2+1}\right)-\frac{Z^2e^2 4\pi\lambda\!\!\!^{-}}{AMc^2}\right]^2\right\}. \quad (17)$$

On can gain more insight into the elastic scattering cross section expected from the absorption cross section by substituting the approximate values $\sigma_m=0.59$ barns, $E_0=13.5$ Mev, and $\Gamma=3.8$ Mev appropriate[21] for $\sigma_a(E)$ in $Au^{197}$. Eq. (16) then becomes:

$$\frac{d\sigma(0°)}{d\Omega}=1.04\frac{\mathrm{mb}}{\mathrm{sr}}\left(\frac{E}{13.5\ \mathrm{Mev}}\right)^2\left\{\left[\frac{1}{L^2+1}\right]^2+\left[\frac{L}{L^2+1}-0.15\left(\frac{13.5\ \mathrm{Mev}}{E}\right)\right]^2\right\}. \quad (18)$$

Slightly better predictions for $d\sigma(0°)/d\Omega$ can be obtained by using the two Lorentz line fit suggested by Fuller and Weiss[21]:

$$\sigma_1=0.255\ \text{barn},\quad E_{01}=13.15\ \text{Mev},\quad \Gamma_1=2.9\ \text{Mev}$$
and (19)
$$\sigma_2=0.365\ \text{barn},\quad E_{02}=13.90\ \text{Mev},\quad \Gamma_2=4.0\ \text{Mev}.$$

(These parameters omit the 5.4% of the observed integrated cross section which is found between 17 Mev and 24 Mev; this omission will not affect the comparison made below.) If the scattering cross section is assumed to have the $(1+\cos^2\theta)$ angular distribution expected for dipole scattering,

$$\frac{d\sigma(135°)}{d\Omega}=\frac{3}{4}\frac{d\sigma(0°)}{d\Omega}. \quad (20)$$

### B. Comparison with Other Experiments

The predictions for $d\sigma(135°)/d\Omega$, obtained by substituting the values of Eqs. (19) and (20) into Eq. (17), were systematically higher than those we obtained experimentally. In order to simplify the comparison of energy dependence, the dispersion prediction is reduced by a factor of 0.82, and shown as the solid curve in Fig. 7. (The 18% reduction is arbitrary and should not be misinterpreted as due to a statistical procedure designed to obtain the best normalization. The particular factor stems historically from an error we made in privately circulated results.[22]) The black dots on Fig. 7 are the experimental points obtained from column 7 of Table I; the errors shown are statistical. The open circles in Fig. 7 are obtained by reducing the earlier experimental scattering values due to Fuller and Hayward[23,24] by the same normalization factor of 0.82.

If the results of the two scattering experiments are compared (without any renormalization), at about 15 Mev the values obtained by Fuller and Hayward[23,24]

[20] E. G. Fuller and Evans Hayward, Phys. Rev. Letters **1**, 465 (1958).

[21] E. G. Fuller and M. S. Weiss, Phys. Rev. **112**, 560 (1958).

[22] This error appears in J. S. O'Connell, thesis, University of Illinois, 1961 (unpublished), and J. S. O'Connell, P. Tipler, and P. Axel, University of Illinois Technical Report 21, 1961 (unpublished). Unfortunately, we probably did not find the error in time to have the correction made in the review article by E. G. Fuller and Evans Hayward to appear in Nuclear Reactions Vol. II, edited by Endt, DeMeur, and Smith.

[23] E. G. Fuller and Evans Hayward, Phys. Rev. **101**, 692 (1956).

[24] The cross sections given in reference 23 were reduced by a factor 0.866 in accordance with reference 15, and they were converted from 120° to 135° by assuming a $1+\cos^2\theta$ distribution. The normalization factor of 0.82, mentioned in the text was also applied.

at 120° are about equal to those we find at 135°. However, given the uncertainties in the absolute cross section, it is probably better to assume a $1+\cos^2\theta$ angular distribution, and to explain the difference by their cross section being 22% too high (or our values being 18% too low). (Of course, the statistical uncertainties of both measurements would admit compromise values without requiring a complete renormalization). In the region of 11.5 Mev, the two experiments disagree somewhat. Although this disagreement is not serious when statistics are considered, its occurrence close to an energy region where the cross section changes relatively rapidly may be indicative of an improper choice of effective mean energy in the poorer resolution experiment.[23]

The implications of the fine agreement above 13.5 Mev between the energy dependence of the measured scattering cross sections and the values calculated from the absorption cross section will be discussed below. The slight discrepancy at about 11.7 Mev and 12.6 Mev, although not outside of statistics, might imply a difference in energy calibration; a shift of about 200 kev would produce excellent agreement. We would not expect so large an energy shift, but cannot exclude about half of this shift because our primary calibration was made at higher values of $E_\beta$ and $E_e$; it is difficult to assess the likelihood of an energy shift in the absorption data which were precise but analyzed in 1-Mev intervals.[21]

## C. Implications of Comparison between Scattering and Absorption Data

There are theoretical and experimental factors which, despite the complications they introduce, give incentives to comparisons between absorption and scattering data. Even though the lack of precision of the experimental data on $Au^{197}$ limit the conclusions which can be reached, the potentiality of such comparisons warrant a brief summary of the relevant factors.

### *1. Improved Accuracy of Absorption Cross Sections*

Measured scattering cross sections can be used to check the absorption cross section with the aid of the rigorous dispersion relations Eqs. (13)–(15), as in Fig. 7. For example, Fuller and Hayward[23] used their measured scattering data to show that there was considerable nuclear absorption at energies above what had been thought to be the giant resonance region in light nuclei. In addition to uncovering such gross errors, precise scattering measurements can be used to calibrate the absolute cross sections in some cases. Elastic scattering experiments have the important advantage of using the same detector to count both the incident and scattered photons. In contrast, absorption cross section measurements involve separate photon and nuclear reaction detectors. Many of these difficulties are discussed by Fuller and Weiss[21] who despite extremely careful measurements on $Au^{197}$ assigned a 10% error to their absolute values. (The 18% reduction of the predictions of the absorption data made in Fig. 7 corresponds to only a 9% reduction in the absolute absorption cross section as indicated in Eq. (16).) Fuller and Weiss[21] used the measured scattering cross sections[23] as a partial check on their absolute cross section values. Another feature of the absorption cross section which can be checked is the difficult correction often used to infer $\sigma(\gamma,2n)$ from the value of $2\sigma(\gamma,2n)$ measured with neutron detectors. The agreement of the dots in Fig. 7 with the predicted curve helps confirm the correction which was made for neutron multiplicity.[21]

### *2. Angular Distribution of Scattered Radiation*

The differential cross section measured at an angle, $\theta$, can be compared with the predicted forward scattering, $d\sigma(0°)/d\Omega$, only if the angular distribution is known. Eq. (20) follows the conventional but unproven procedure of assuming pure dipole scattering. If the scattering were pure quadrupole, $d\sigma(135°)/d\Omega$ would be expected to be smaller by a factor of 3. (The possibility of quadrupole scattering and the obvious possibility of an error in absolute cross section are the only ones which can explain a measured scattering cross section at 135° below the prediction based on absorption; several other factors to be discussed below can explain scattering cross sections which are too high.) If quadrupole scattering plays any role, it would probably contribute differently at different energies (e.g., the low points at 11.66 Mev and 12.64 Mev might be due to some quadrupole scattering at these energies).

If the scattering were isotropic, $d\sigma(135°)/d\Omega$ would be larger than that implied by dipole scattering by a factor of $\frac{4}{3}$. Angular distributions considerably more isotropic than $(1+\cos^2\theta)$ would be expected if the different spin states reached by dipole absorption were isolated rather than part of a continuum. For this reason, if the possibility of quadrupole scattering were eliminated, the experimental scattering cross sections at 11.66 Mev and 12.64 Mev would give direct experimental evidence that in this energy region in $Au^{197}$ levels with spins $\frac{1}{2}$, $\frac{3}{2}$, and $\frac{5}{2}$ overlap and participate in photon scattering. In view of other factors which can cause discrepancies to arise in the comparison of scattering and absorption data, it would be worthwhile to obtain independent experimental values of the angular distribution of scattered photons.

### *3. Errors Caused by Fine Structure in the Absorption Cross Section*

Fine structure in the energy dependence of the absorption cross section may introduce error[23,25] because the available measured values [which are substituted into Eqs. (11) and (13)] are poor resolution averages.

[25] A. S. Penfold and E. L. Garwin, Phys. Rev. **116**, 120 (1959).

When the average rather than the actual absorption cross section is used, not only will the proper detailed energy dependence fail to appear in calculated values of $d\sigma(0°)/d\Omega$, but the predicted average value of $d\sigma(0°)/d\Omega$ will be low. Thus, an average experimental scattering cross section which is larger than that predicted may indicate unresolved structure in the absorption cross section. This effect has been used by Penfold and Garwin[25] to confirm the reported fine structure in photoabsorption by $O^{16}$, and to cast doubt on such structure being present in $C^{12}$. The scattering at 11.66 Mev and 12.64 Mev can thus be used as evidence that the levels in $Au^{197}$ overlap in this energy region.

### *4. Possible Dependence of Absorption Cross Section on Nuclear Orientation*

The measured values of both the scattering and absorption cross sections are usually averages over both the orientations of the target nuclei and the polarizations of the incident photons. If the photonuclear process depends on the relative orientation of the nuclear spin and the photon polarization (i.e., if the nucleus has a tensor polarizability) the implied scattering cross section would be increased.[20,26,27]

When the nucleus has a tensor polarizability, the elastic scattering cross section implied by an observed absorption cross section depends on the spin of the scattering nucleus. For a nuclear spin of 0 or $\frac{1}{2}$, the direction of photon polarization can play no role, and the expected elastic scattering can be calculated from the equations given above.[26] For higher values of the nuclear spin, the calculated elastic scattering becomes larger due to tensor polarizability;[26,27] in the limit of very high spin, the expected results[26,27] would be those obtained by a classical average over relative orientations.[20]

Experimental verification of the effects of tensor polarizability on pure elastic scattering is somewhat complicated because the measured scattered events can include high energy inelastic gamma rays as well as elastically scattered gamma rays. The inelastic scattering of photons to the very low lying rotational excitations of the ground state in highly deformed nuclei has been calculated[27,28] with the aid of a particular nuclear model. The main assumptions in the calculation are that there are pure low lying rotational states, and that the photonuclear excitations in particular subregions of the giant resonance can be associated with either $\Delta K=0$ or $\Delta K=\pm 1$. (These calculations omit the possibility of inelastic scattering leading directly to low lying excited intrinsic levels). According to these calculations the sum of the elastic scattering and inelastic scattering to the ground state rotational levels is a constant independent of nuclear spin.[27] The enhancement predicted over that given by the above equations has a distinctive energy dependence which makes it possible to separate this enhancement from relative errors in absolute cross sections.

Experimental results by Fuller and Hayward on Ta, Er, and Ho have shown enhancements in the scattering cross section which had the correct energy dependence to be explained by tensor polarizability combined with inelastic scattering to rotational levels.[27] The available theories do not predict any similar effects for spherical nuclei such as $Au^{197}$. (Treating the Fuller and Weiss parameters[21] as indicative of slight deformation implies a scattering cross section almost the same as that shown in Fig. 7; the maximum difference at any energy is less than 7%.) On the other hand, it is conceivable that there are other sources of tensor polarizability.

### *5. The Effects of Inelastic Scattering*

Due to the poor energy resolution of the gamma ray detector, high energy inelastically scattered gamma rays cannot be distinguished from elastically scattered gamma rays. If there were appreciable high energy inelastic scattering, the observed cross sections should be greater than the predicted elastic scattering cross sections. A comparison between measured scattering and calculated elastic scattering could provide valuable new information about the probability of high energy inelastic scattering.

There are very few experimental determinations of high energy inelastic scattering. Stearns[29] inferred significant high energy inelastic scattering for Cu, Sn, Pb, and Bi but these inferences are highly questionable in view of what is now known about the energy dependence of elastic scattering. (Stearns used a 5 cm×7 cm NaI crystal with quite poor energy resolution to detect the scattering of unresolved 15-Mev and 17.6-Mev gamma rays obtained by bombarding Li with protons. The conclusion that significant inelastic scattering existed was based on there being more lower energy pulses in the scattered spectrum that in the direct spectrum. At least in the cases of Pb, and Bi, elastic scattering alone could explain such a shift toward lower energies.) Penfold and Garwin[25] have reported evidence for inelastic scattering to energy levels at higher excitations; such inelastically scattered photons would be of an energy distinguishable from elastically scattered photons.

A different type of inelastic scattering has been measured[30,31] for $Au^{197}$ by detecting the photoproduction of $Au^{197m}$. This reaction would represent a sum of all

[26] A. M. Baldin, J. Exptl. Theoret. Phys. (U.S.S.R.) **37**, 202 (1959); [translation: Soviet Phys.—JETP **10**, 142 (1959)].

[27] E. G. Fuller and E. Hayward in *Proceedings of the International Conference on Nuclear Structure, Kingston,* (University of Toronto Press, Toronto, Canada and North-Holland Publishing Company, Amsterdam, 1960); see pp. 760–766.

[28] Z. Maric and P. Möbius, Nuclear Phys. **10**, 135 (1959).

[29] M. B. Stearns, Phys. Rev. **87**, 706 (1952).

[30] A. G. W. Cameron and L. Katz, Phys. Rev. **84**, 608 (1951).

[31] Luise Meyer-Schützmeister and V. I. Telegdi, Phys. Rev. **104**, 185 (1956).

gamma ray cascades which lead to the isomer. Peak cross sections of[30] 5 mb and[31] 2 mb were obtained at 15 Mev. These values could serve as a guide to the total inelastic scattering due to low energy photon cascades if complicated spin-dependent corrections[32] were made. However, there is no credible connection between the compound-nuclear photon cascades and the high energy inelastic gamma rays which, if they are numerous, would be due to direct interaction.

The inadequacy of experimental data on high energy inelastic scattering is matched by a complete fuzziness of photonuclear theory[33] on this subject. Existent theories do not assign a significant role to valence nucleons in the giant resonance photoabsorption. A doubly magic nucleus with a zero spin, positive parity (0+) ground state can serve well as the prototype for existing theories; the giant resonance would then be a 1− state. If, as in the case of $Au^{197}$, the ground state is $\frac{3}{2}+$, the dipole excitation would presumably reach $\frac{1}{2}-$, $\frac{3}{2}-$, and $\frac{5}{2}-$ states which can be thought of as produced by the coupling of the $\frac{3}{2}+$ valence nucleons to the basic 1− giant resonance state. It would also be expected that if $Au^{197}$ nuclei were obtainable in the $\frac{1}{2}+$ first excited state (at 77 kev), giant dipole photoabsorption would lead to $\frac{1}{2}-$ and $\frac{3}{2}-$ states. There is no obvious reliable way to estimate whether the $\frac{1}{2}-$ and $\frac{3}{2}-$ states produced by dipole excitation of the $\frac{3}{2}+$ ground state mix sufficiently with the corresponding states produced by dipole excitation of the $\frac{1}{2}+$ state to imply considerable inelastic scattering. The two types of $\frac{1}{2}-$ or $\frac{3}{2}-$ states certainly mix thoroughly by the time the compound nucleus model applies; but it is difficult to predict theoretically to what extent this mixing occurs while the giant dipole state maintains the special coherence it needs to emit elastic gamma rays.

### D. Conclusions

The simplest interpretation that can be given to the agreement shown in Fig. 7 after normalization is that either the scattering cross sections are too low by 22% or the absorption cross sections are too high by 9%; of course, statistical errors admit smaller absolute errors and a compromise value. This conclusion would imply that the scattering was mainly dipole, that the absorption cross section had no fine structure, and that the high energy inelastic scattering was negligible. On the other hand, particularly in view of the large statistical errors and the possible systematic errors, other interpretations are possible.

If experimental errors have made the scattering appear even higher (i.e., if a more accurate version of Fig. 7 would show the dots below the curve), the most likely explanation would be that $d\sigma(135°)/d\Omega$ was less than $\frac{3}{4}d\sigma(0°)/d\Omega$ (as was assumed in Fig. 7). Quadrupole scattering could give such an effect.

On the other hand, a variety of factors could explain the "scattering" dots falling above the curve based on absorption. The possibilities include: (1) an angular distribution for scattering in which $[d\sigma(135°)/d\Omega]/[d\sigma(0°)/d\Omega]$ is more than $\frac{3}{4}$, (2) unresolved find structure in the absorption cross section, (3) tensor polarizability, and (4) high energy inelastic scattering.

### ACKNOWLEDGMENTS

Our confidence in the results reported in this paper was bolstered by results obtained in other experiments performed after improvements had been made in the monochromator. One of us (P. T.) and Nelson Stein studied and improved the betatron performance. The electron optics were tested with the aid of Li ions by Dr. David Sutton, Miss Franca Kuchnir, and Kongki Min. Improvements in the betatron energy regulator and in the electron scalers were made by Herbert Kuehne.

We wish to thank Professor A. O. Hanson, Dr. D. Jamnik, and Dr. H. E. Hall, who were initial collaborators in the development of the monochromator. (This group had initially planned to use the equipment to measure inelastic electron scattering and therefore participated in the design, construction, and testing of essentially all of the apparatus.) We also wish to thank Professor J. Goldemberg who participated in some of the very early stages of development.

We are also glad to acknowledge the aid of J. Kanz, H. Kuehne, and J. Moyzis in testing, in computing, and in taking the final data. We were also aided by the service staff of the Physics Research Laboratory including particularly E. R. Cordes who built and improved the designs of the dispersion and spectrometer magnets, James Harlan and his electronic shop staff, W. M. Henebry who designed and tested the initial energy stabilizing system for the betatron, and the betatron engineers, Robert Wardin and Roger Lilly, who together with the betatron operating crew made possible the rigorous operating schedule.

[32] J. R. Juizenga and R. Vandenbosch, Phys. Rev. **120**, 1305 (1960).

[33] See D. H. Wilkinson, Ann. Rev. Nuclear Sci. **9**, 1 (1959) for a recent review of the photonuclear theories; the important extensions made to the independent particle model interpretation by G. E. Brown and M. Bolsterli [Phys. Rev. Letters **3**, 472 (1959)] and by G. E. Brown, L. Castillejo, and J. A. Evans. [Nuclear Phys. **22**, 1 (1961)] do not contribute significantly to the inelastic scattering problem.